437 MHz Directive antenna for double CubeSat

Erik Narverud

January 16, 2007

Abstract

This report describes the idea, theory, work and results of an antenna concept developed for a double CubeSat satellite. The goal of the work was to create a computer model of an optimized antenna design, conforming with the design specifications. Although attention is given to to both mechanical and electrical aspects of the design, the primary effort relates to the electrical properties. For a more extensive discussion regarding the mechanical aspect, the report concerning the 145 MHz antenna [2] can be consulted.

Contents

List of Figures

List of Tables

Chapter 1

Introduction

The idea of implementing a directive UHF-antenna on the newly proposed student satellite came from the need for a high-speed data link, able to transmit a VGA imagedown to earth in a single pass. This would require a robust downlink of at least 9600 baud, preferably incorporating FEC. As the satellite will be stabilized, a directive antenna was suggested in order to increase channel capacity. The 437.305 MHz and 145.98 MHz carrier frequencies were chosen as communication channels, due mainly to their vacancy caused by the failure of the NCUBE missions. The reason why the 437 MHz antenna was chosen to be the directive one, was partially inspired by the satellite itself. The increased length of the double CubeSat frame, in comparison to the single cube, meant that a quarter-wavelength antenna solution could be implemented on the chassis. This was not possible with the 145 MHz band. The solution was inspired by the Yagi-Uda antenna, with it's reflector mounted a quarter of a wavelength behind the radiating dipole. The chosen design is, in fact, a two-element Yagi-Uda antenna, mounted vertically on the satellite, with a nadir-directed main lobe. In contrast to the normal Yagi-Uda, however, the chosen solution does not make use of directors in front of the dipole, as these would be difficult to implement. However, such directors are not necessarily wanted anyway, as maximum directivity is not the primary concern of the antenna design.

Chapter 2

Theory

2.1 Concept

As mentioned, it was the Yagi-Uda endfire array, such as the one shown in figure 2.1, which first spawned the idea of using a passive reflector element to

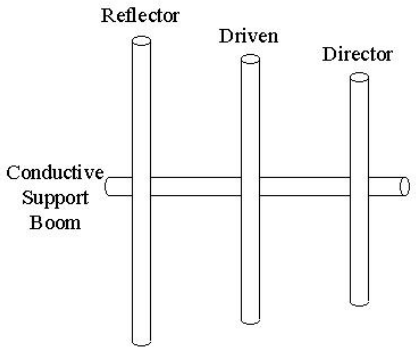

Figure 2.1: Simple three-element Yagi-Uda array antenna

obtain directivity. However, the antenna does not make use of any directors such as the Yagi-Uda antenna does, as these can not be fit on the satellite without the use complicated mechanics for folding and stowing. Besides, according to [1], the directivity in a Yagi antenna increases with the number of directors, so removing the directors should contribute to widening the lobe, which is desirable. What remains after removing these elements, as well as the center conductor of the Yagi, is, in essence, a dipole mounted horizontally over a thin, parallel, conducting plane. The distance between the ground plane and the dipole is close to one quarter of a wavelength, resulting in a wave propagation illustrated in figure 2.2.

The principle can be summed up as follows: Waves initially propagate as from a regular dipole, traveling uniformly out from the parallel axis of

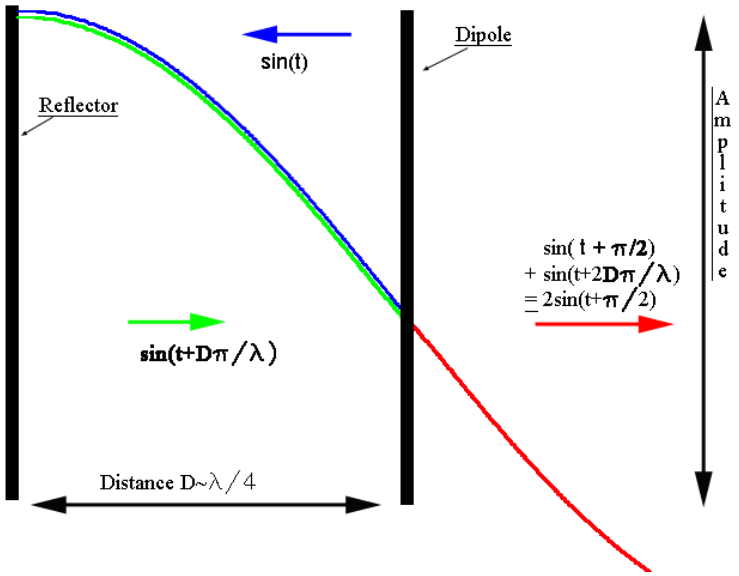

Figure 2.2: Conceptual illustration of the wave propagation. Note that the red wave is a sum of the reflected wave and a wave emitted later in time.

the dipole. However, the part of the radiation propagating backwards will reach the reflector element and be reflected back toward the dipole. When the reflected wave reaches the dipole, it will have traveled 1/2 wavelength, having changed it's instantaneous phase by π radians. During this time, the dipole current has also changed it's phase by π radians, resulting in a constructive interference of waves traveling in the opposite direction of the reflector. This largely describes how the antenna works, and how it was treated during the design process. Further theory can be found in [1], chapter 4.7.5. Two important differences from an ideal dipole should be be noted: First, because of the mechanical implementation, both the dipole elements and the reflector are realized as flat sheet metal, similar to steel measuring tape. Secondly, the reflector creates a capacitive coupling with the dipole, altering it's ideal resistance.

2.2 Satellite coverage area

Because a LEO satellite orbits the earth in less than two hours, any ground station trying to communicate with the satellite will need either a wide-lobe, low-gain antenna, or a steerable main lobe able to track the satellite, due to the fact that the satellite crosses the visible sky over the ground station in only ten or fifteen minutes. The same goes for the satellite; If a high-directivity antenna is incorporated, the main lobe must be steerable in order to keep a ground station in sight. In the case of a small LEO satellite as

discussed in this project, it cannot be expected that the satellite attitude will be controlled very exactly, and a steerable main lobe antenna (using a phased array, for example) would therefore be very difficult to operate. If the UHF- band is to be used, such an array would sequestrate to much space to be practical in the case of a satellite based on the CubeSat standard.

Although only one station is to communicate with the satellite at any given time, a large coverage area implies that communication can take place even though the satellite is not directly overhead, enabling a larger number of transmissions per day. According to [5], a satellite orbiting at 750 km will have a scan angle of $\pm$ 57.2°, provided a minimum elevation of 20° at the ground station. This will correspond to a coverage area of $\pm$ 12.8° in latitude and longitude, assuming that the satellite antenna is pointing directly toward the earth. This assumption must not be made hastily, however, as this particular satellite may not have the benefit of accurate attitude management. This means that the satellite may be slanting, thus reducing the received signal power. Also, if the satellite is spinning around it's nadir axis, the main lobe will rotate with it, and if the lobe has large gain differences, the signal strength will fluctuate with the rotation. All these facts leaves us with the main design goals; To maximize radiated power in the nadir direction, while keeping the main lobe as wide and uniform as possible.

2.3 Mechanical characteristics

The mechanical characteristics of the antenna must conform with the given specifications, thus severely reducing the degrees of freedom available in the design. The biggest challenge mechanically is the design of a simple, robust, computer controlled release mechanism. It must be capable of holding the antennas in place during launch, while releasing them with absolute certainty at the correct moment. The antenna must not be allowed to release when inside the P-POD, or upon initial release, as this may cause the satellite to get stuck, or damage the carrier satellite. The mechanism solution most relevant to this antenna is the use of nylon threads fastened in the ends of the elements. The elements themselves can then be fashioned as thin, foldable sheets of metal. The report concerning the 145 MHz antenna [2] goes into deeper detail about such a release mechanism, the concepts being quite similar for both antennas.

As the antenna needs to have about 170 mm of space between the dipole and the reflector, the possible mounting solutions reduce to two main categories, shown in figures 3.5 and 3.6. The antenna may be mounted in the center of the satellite, with the reflector and dipole being partially embedded in the structure, or on the outside of the front sidewall, from now on referred to as the *center* and *offset* solutions, respectively. Both types allow for a small amount of position adjustment, and the principal, physical differences

between them will be found in the release mechanism and the stowing solution. Because the offset solution is restrained by the 6.5 mm of space allowed by [3], the center solution may allow for wider elements, resulting in a more rigid design. On the other hand, the center solution may be more prone to interference with the solar panels, and it might be more difficult to realize as it may come in conflict with internal modules.

2.4 Electrical characteristics

There are some important factors to consider in order to get the maximum efficiency from an antenna, all depending on the various dimensions of the antenna structure. One is the *Voltage Standing Wave Ratio*, or $VSWR$, shown mathematically in equation (2.3). This is a number describing to which extent the antenna matches the feeding network, and is therefore closely related to the power radiated from the antenna. A small $VSWR$ means that little power is returned back into the feeding network from the antenna, implying that most of the power is converted into radiation. In other words, if the $VSWR$ is good, the *Return Loss*, R_L, will be small. This can bee seen from the definition of the *antenna resistance*, defined in equation (2.1).

$$R_A = R_r + R_L \tag{2.1}$$

Here, R_r is the *radiation resistance* of the antenna, in other words, the part of R_A corresponding to the radiated power. The definition of R_A implies that when R_L is minimized, $R_A = R_r$. As R_r is a hypothetical resistance derived from the power consumption of an antenna, all power fed to the antenna will ideally be converted to radiation if R_L is zero. As seen from equation (2.2), this will yield a *reflection coeficcient*, Γ, of zero, and the maximum radiation efficiency will therefore correspond to a $VSWR$ of unity.

$$\Gamma(f) = \frac{Z_L(f) - Z_0}{Z_L(f) + Z_0} \tag{2.2}$$

$$VSWR(f) = \frac{1 + |\Gamma(f)|}{1 - |\Gamma(f)|} \tag{2.3}$$

It is important to notice that a $VSWR$ of 1 does not neccesarily mean that all the power fed to the antenna is emitted as radio waves. A small part of the energy will always be converted into heat, due to ohmic losses in the antenna. How much is dependent on the conductive properties of the antenna materials.

The *Directivity*, D, of the antenna is another important factor. It is defined by [4] as the relation between the maximum and average radiation intensity of the antenna, shown mathematically in equation (2.4):

$$D = \frac{U_{max}}{U_{av}} = \frac{4\pi U_{max}}{P_r} \tag{2.4}$$

Here P_r is the total radiated power. This can be related to the input power $P_i = P_r + P_l$ of the antenna through the formula for R_A, p_l being the power loss corresponding to R_L. According to [4], If P_i is used instead of P_r, the *Power Gain*, G_p, replaces D in equation (2.4). Hence, the *Radiation Efficiency* η_r can be derived directly as the ratio of G_P to D:

$$\eta_r = \frac{G_p}{D} = \frac{P_r}{P_i} \tag{2.5}$$

The bandwidth of the antenna can be found by calculating or measuring the $VSWR$ for several frequencies. Because the antenna impedance changes with frequency, the antenna will only be efficient for a certain area of the frequency spectrum. Usually, the bandwidth is defined as the frequency area having a $VSWR$ of less than 2.

As stated previously, although the antenna is supposed to be directive, *maximizing* the directivity is not the main goal, as this would correspond to a very narrow main lobe. However, it is important to minimize the unwanted sidelobes. [1] states that the number of lobes N_l emitted from a dipole over a perfectly conducting, infinite plane is roughly dependent of the distance h between the dipole and the plane:

$$N_l \approx 2(\frac{h}{\lambda}) \tag{2.6}$$

As seen from equation (2.6), for $h = \frac{\lambda}{4}$, $N_l \approx \frac{1}{2} \approx 1$. Thus, only one lobe, radiating away from the reflector, can be expected. This is for an infinite plane, however, and in reality some energy will be radiated backwards through the reflector. The directivity is therefore important in order to show how much energy is radiated in the correct direction, and how much is radiated in the wrong direction.

To get a better understanding of how wide the main lobe is, the *3 dB angle* is used. This is a measure of the width of the main lobe, and is defined as the opening angle in the maximum gain direction, where the lobe magnitude has decreased by half (hence the term "3dB"). In other words, if the radiation intensity has been decreased by half in an angle of α° from the direction of maximum intensity, and the lobe is uniform, the 3dB angle will be $\alpha_{3dB} = 2\alpha$. In the case of a dipole, the lobe will be elliptical in shape. Therefore, two 3dB angles must be measured in order to describe the lobe. The relation between the two angles gives information about the uniformity of the lobe, and ideally they should be identical.

The different factors described above are key elements in deciding if the antenna is matching the design goals. Although the simplified wave propagation of a dipole over an infinite conducting plane can be said to match the propagation behavior of the antenna, the mathematical relations are not corresponding. This is clearly seen when comparing the theoretical calculation of the radiation resistance to simulated values, as shown below. On

page 201, [1] shows that, in the case of a perfectly conducting, infinite plane as a reflector, P_r can be expressed as:

$$P_r = \eta\frac{\pi}{2}\left|\frac{I_0 l}{\lambda}\right|^2\left[\frac{2}{3} - \frac{sin(2kh)}{2kh} - \frac{cos(2kh)}{(2kh)^2} + \frac{sin(2kh)}{(2kh)^3}\right] \tag{2.7}$$

Here, $k = \omega\sqrt{\mu\epsilon}$ is the wavenumber, η is the free space impedance, I_0 is the current and l is the length of the dipole. R_r can be derived directly from the relation $P_{rad} = \frac{I_0^2}{R_r}$. When substituting for R_r in equation (2.7) and inserting ideal values, i.e. $\eta = \eta_0 = 120\pi$, $l = \frac{\lambda}{2}$, $h = \frac{\lambda}{4}$ and $k = \omega\sqrt{\mu_0\epsilon_0} = \frac{2\pi f}{c}$, (2.7) reduces to

$$R_r = 30\pi^2\left[\frac{2}{3} - \frac{sin(\pi)}{\pi} - \frac{cos(\pi)}{\pi^2} + \frac{sin(\pi)}{\pi^3}\right] \approx 227\ \Omega \tag{2.8}$$

This is considerably higher than the 73.1 Ω resistance of an ideal dipole. One might therefore expect that the radiation resistance should increase in the event of a reflector being introduced. Simulations showed that this was not the case, as the resistance was actually somewhat reduced. In fact, when values from a simulation giving an input resistance of 50 Ω was inserted into the equation, this gave an answer of over 158 Ω. There was clearly no coherence between the theoretical and practical case, and further theoretical studies were therfore abandoned in favor of a more extensive simulation.

Chapter 3

Design process and results

3.1 Design method

Instead of relying on mathematical descriptions, an empirical test procedure was created to effectively tune the antenna. It was hoped that the antenna could be tuned to optimum performance and still comply with the mechanical restrictions. Using the simulation software $WIPL-D$, a dipole with a parallel reflector, realized as infinitely thin, perfectly conducting sheets of metal, was created. The layout and the adjustable dimensions are shown in figure 3.1. The dimensions were varied, one by one, in order to gain an

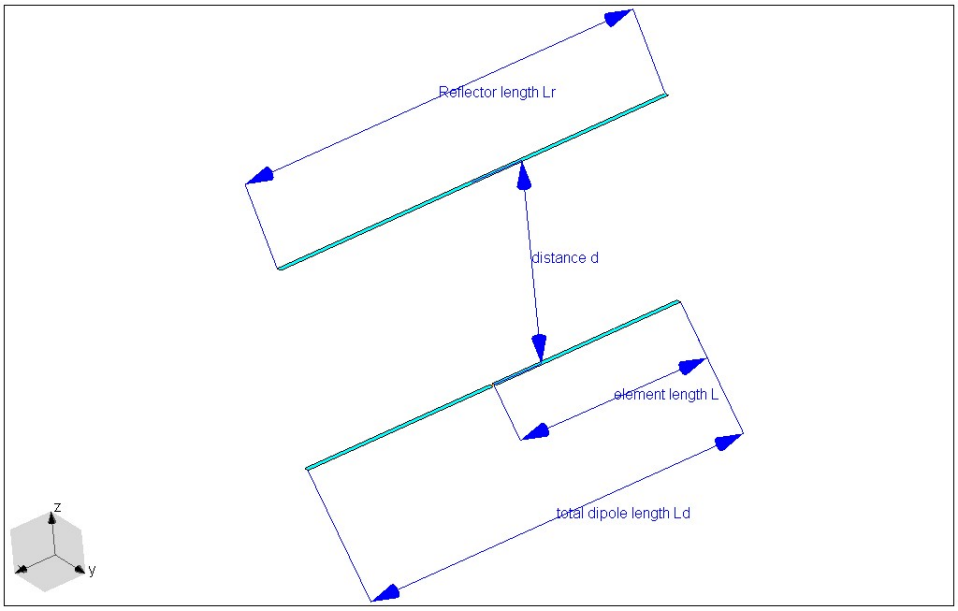

Figure 3.1: The antenna layout with the adjustable dimensions

understanding of how they affected the electrical properties of the antenna.

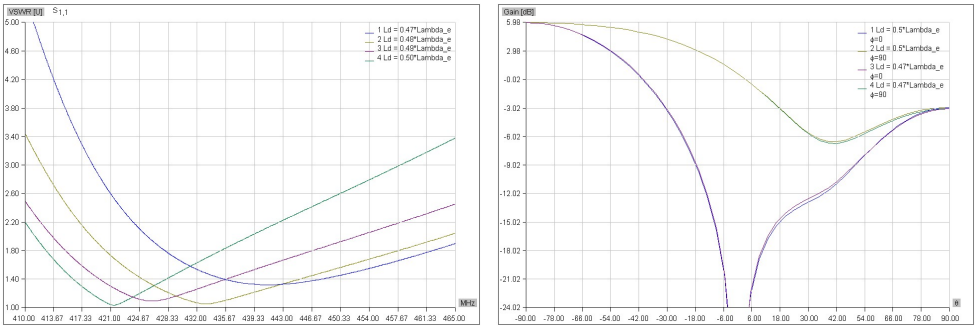

Figure 3.2: VSWR and radiation patterns for various dipole lengths

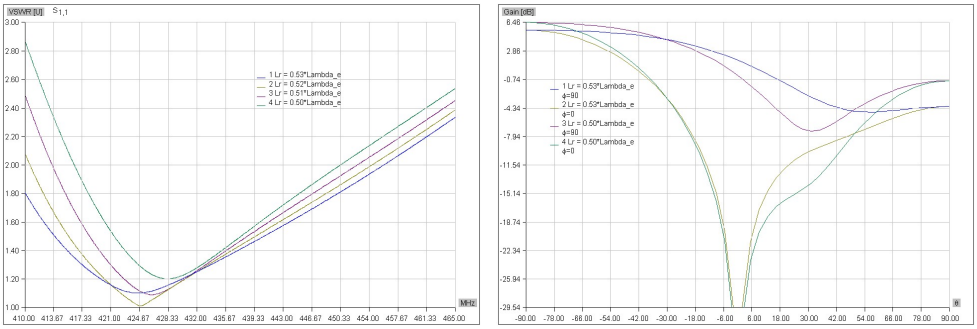

Figure 3.3: VSWR and radiation patterns for various reflector lengths

The values were limited by the wavelength and the mechanical restrictions. The width of the sheet elements, however was set to a constant 4 mm, due to the restricted space available for the offset mounting solution. Also, the feeding gap between the dipole radiators was set to 2 mm, making the total dipole length $L_d = 2L + 2$ mm at all times. The default values used were chosen as the Yagi-parameters given in [4], page 649. Here, the dipole length $Ld = 0.49\lambda_e$, the reflector length $Lr = 0.51\lambda_e$ and the distance $d = 0.25\lambda_e$. Here, $\lambda_e \approx 661$ mm is the electrical wavelength, found by optimizing the length of the dipole without the presence of the reflector. As these values are given for a Yagi-Uda antenna incorporating directors, they were not assumed to be ideal. The reason for using them was simply to have a reasonably correct wavelength relation. Figures 3.2, 3.3 and 3.4 show how some key electrical values depend on the various parameters.

The behavior of the electrical properties in relation to change in the physical parameters, is summed up in table 3.1.

The tuning of the various dimensions was based on these initial simulation results. As mentioned, they were performed without the presence of any support structure, such as a satellite chassis. However, it was believed that the satellite chassis would interfere considerably with the radiation pat-

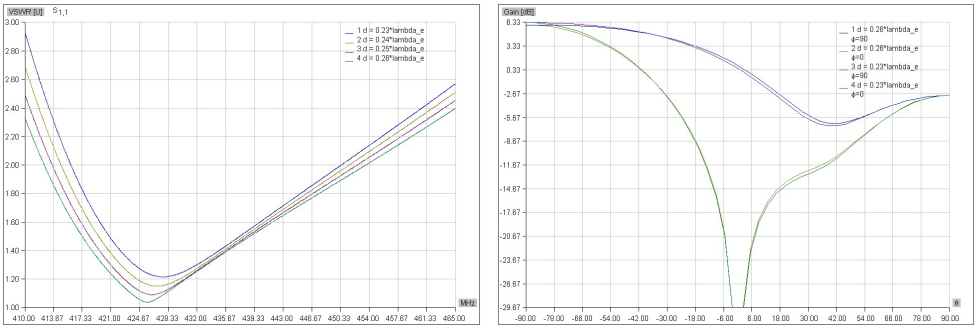

Figure 3.4: VSWR and radiation patterns for various distances between dipole and reflector

variable **action**	*dipole length Ld* *increases*	*reflector length Lr* *increases*	*distance d* *increases*
directivity	≈ constant	decreases	decreases
lobe width	≈ constant	increases	≈ constant
uniformity	≈ constant	decreases	≈ constant
center frequency	decreases	≈ constant	≈ constant
$\|impedance\|$	increases	≈ constant	increases
bandwidth	decreases	increases	≈ constant

Table 3.1: Relation between electrical and physical attributes

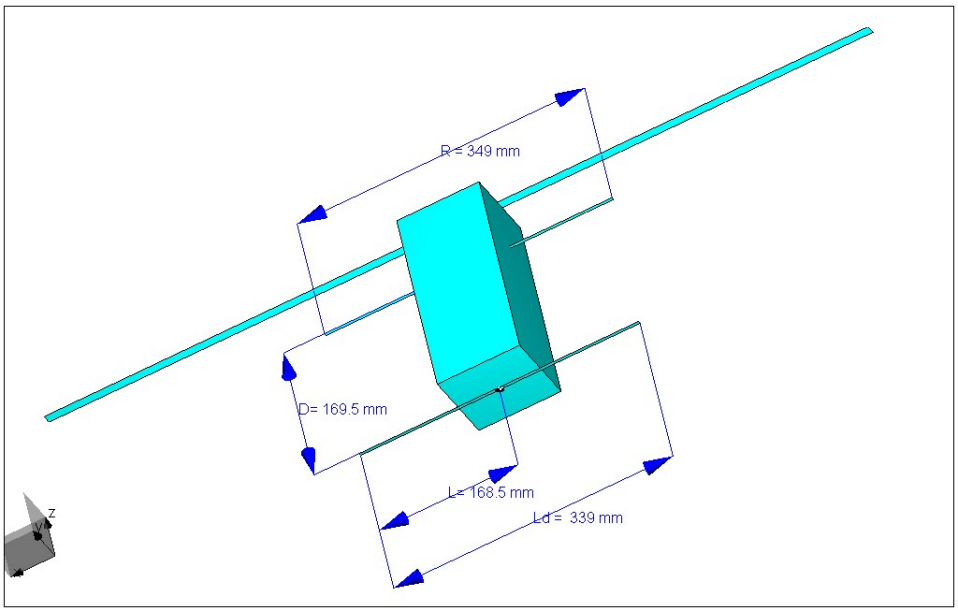

Figure 3.5: Layout of the center-mounted solution. The values shown are for the final, optimized antenna

tern of the antenna, because of their closely matching dimensions and the conducting frame and solar panel-clad surfaces. It was therefore decided to simulate the satellite structure as a perfectly conducting box, simplifying the design effort considerably. The end result was two simulation setups, one for each mounting solution, shown in figure 3.5 and 3.6. As one can see from the figure, the 145 Mhz antenna is also included in the simulation. In both cases, 1 mm of space was allowed between the box and the dipole elements, in order to reduce the impact of the chassis on the antenna properties.

Both the center and offset solutions were tuned to optimal performance, and compared in order to see which solution gave the best performance. The simulations showed that the offset antenna solution could be tuned to an exact 50 Ω match, while the center-mounted solution only reached a $VSWR$ of 1.28, with a center-frequency impedance of about 60 Ω. The center-mounted solution also had a more elliptical lobe and conciderably lower gain for the entire coverage area. These results, in addition to a higher mechanical complexity, ruled out the center-mounted solution, and the side-mounted solution became subject for further simulations.

After the side-mounted solution had been fully optimized, a simulation was run with the reflector folded down, while the dipole remained extended. A layout of this setup is shown in figure A.5 in appendix A. A simulation was also performed with both reflector and dipole folded, to see if the antenna would work even if the release mechanism would fail.

After the desition had been made to go forward with the side-mounted

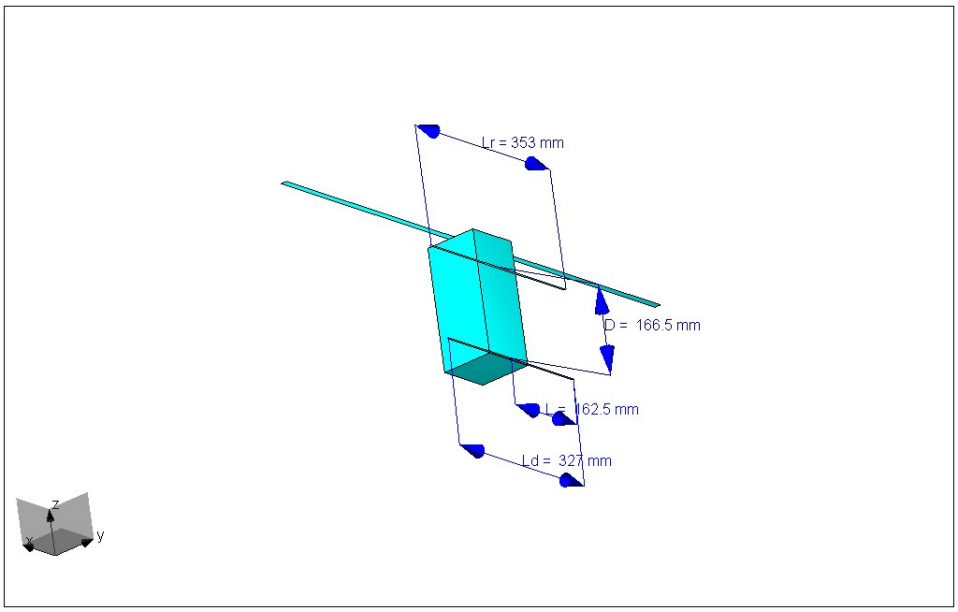

Figure 3.6: Layout of the offset solution. The values shown are for the final, optimized antenna

solution, the Autocad 3D drawing, shown if figure 3.13, was made to control that there would be enough space available for the antenna. Then, a physical chassis model, shown in figure A.8 was made in accordance with the mechanical specifications, in order to confirm the CAD results. To be able to use the model for antenna measurements, the model was fitted with circuit boards as sidewalls, and the antennas, made from carpenters tape, were installed as accurately as possible. An LNA coax connector was mounted on the inside of the PCB, directly behind the dipole center, and feeding wires were soldered on, connecting the elements with the coax connector. Thus, the antenna could be fed directly from a signal generator or network analyzer for electrical testing. Unfortunately, there was not enough time, nor equpiment or aid from the institute, to perform any physical measurements before the report deadline. However, as work will be done on closely related topics, tests are expected to be carried out during the spring of 2007.

3.2 Simulation Results

The resulting antenna layout is as given in figure 3.6. The key values are given in table 3.2. Note that 1 mm of space has been allowed between the antenna and chassis sidewall. Also, the dipole is situated in the *nadir plane*, in other word as far down on the satellite as possible, right on the edge of the box.

Attribute	**Name**	**Value**	**unit**
dipole length	L_d	327	mm
dipole element length	L	162.5	mm
dipole width	W_d	4	mm
feed gap	$Ld - 2L$	2	mm
reflector length	L_r	353	mm
reflector width	W_r	4	mm
Distance between dipole and reflector	D	166.5	mm
clearance between chassis and antenna		1	mm
chassis width		100	mm
chassis length		100	mm
chassis height		227	mm

Table 3.2: Key attributes with values for the optimized design

The radiation pattern for the optimized antenna is shown in figure 3.7 and 3.8. Radiation in the four main horizontal directions are given in figure 3.9. An important result is the edge gain of different scan angles, shown in figure 3.10. Here, the normalized gain is given in dB, and one should note the gain of the 110° scan angle, giving the worst case gain corresponding to a 20° elevation. As one can see, the pattern is somewhat distorted by the structure, giving a small sidelobe pointing upwards through the satellite. This also contributes to streching the main lobe, a feature that is clearly visible in the scan angle plots. Figures 3.11 and 3.12 show the standing wave ratio and smith chart for the usable bandwidth of the antenna. As seen, the antenna is a near perfect 50 Ω match at the center frequency of 437.305 MHz. The main electrical characteristics of the antenna are given in table 3.3. Some key values are also given for the antenna with the reflector folded. Plots of radiation pattern and VSWR for this particular case are given in figures A.6 and A.7.

As the center-mounted solution was not given any further investigation during the simulation process, the measurement results for this antenna will not be given in detail. However, a comparison of the simulated VSWR and radiation patterns are given in figures A.1, A.2 and A.3. No results are given for the case when both dipole and reflector are folded, as this rendered the antenna totally unusable.

The physical chassis model, with offset antenna solution and coax plugs mounted, is shown in figure A.8 in appendix A. The folding solution can be studied in greater detail in the CAD drawing shown in figure 3.13.

Attribute	**Name**	**Value**	**unit**
Center frequency	f_c	437.305	MHz
WSVR at f_c	$WSVR(f_c)$	≤ 1.01	-
required bandwith	B_r	≈ 0.05	MHz
effective bandwith	B	32	MHz
impedance at f_c	$\lvert Z_{1,1}(f_c)\rvert$	50	Ω
min impedance	$\lvert Z_{1,1}(428MHz)\rvert$	38.5	Ω
max impedance	$\lvert Z_{460MHz}\rvert$	87.25	Ω
average impedance change	$\delta \lvert Z_{1,1}\rvert / \delta f$	1.52	Ω/MHz
main lobe gain (directivity)	D	5.77	dB
reverse lobe gain	D_r	-3.2	dB
largest 3 dB angle	$\alpha_{3dB,max}$	151	deg
smallest 3 dB angle	$\alpha_{3dB,min}$	76	deg
max gain variation at 110° scan angle	ΔG_{110}	7	dB
max gain variation at 80° scan angle	ΔG_{80}	≈ 3	dB
with folded reflector			
Center frequency	$f_{c,folded}$	439	MHz
VSWR at $f_{c,folded}$	$WSVR(f_{c,folded})$	≤ 1.56	-
VSWR at f_c	$WSVR(f_c)$	≈ 1.8	-
effective bandwith	B_{folded}	≈ 5	MHz
impedance at $f_{c,folded}$	$\lvert Z_{1,1}(f_{c,folded})\rvert$	31.69	Ω
impedance at f_c	$\lvert Z_{1,1}(f_c)\rvert$	≈ 40	Ω

Table 3.3: Key attributes for the optimized design

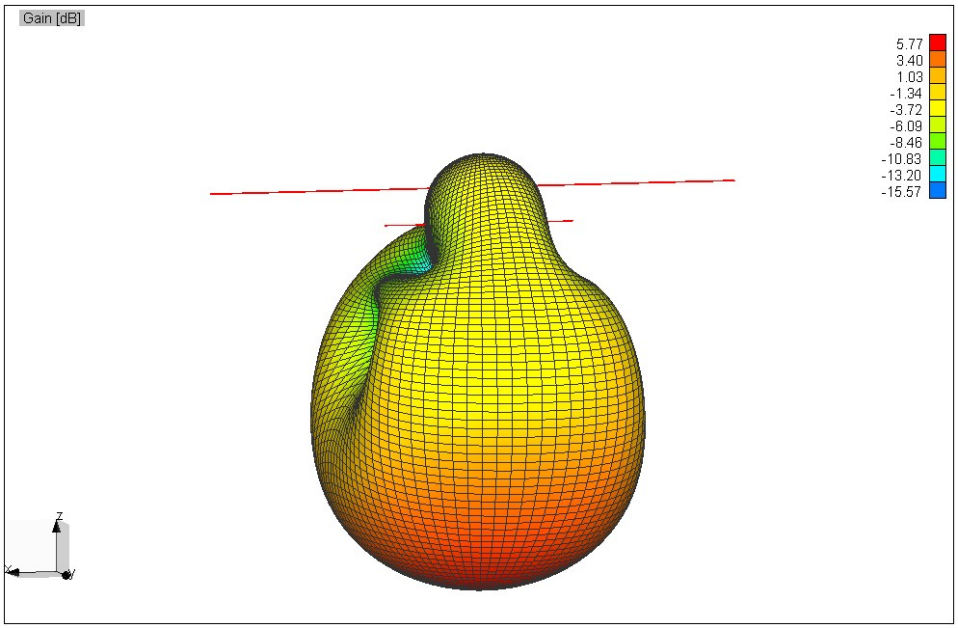

Figure 3.7: Radiation pattern of the dipole in dB.

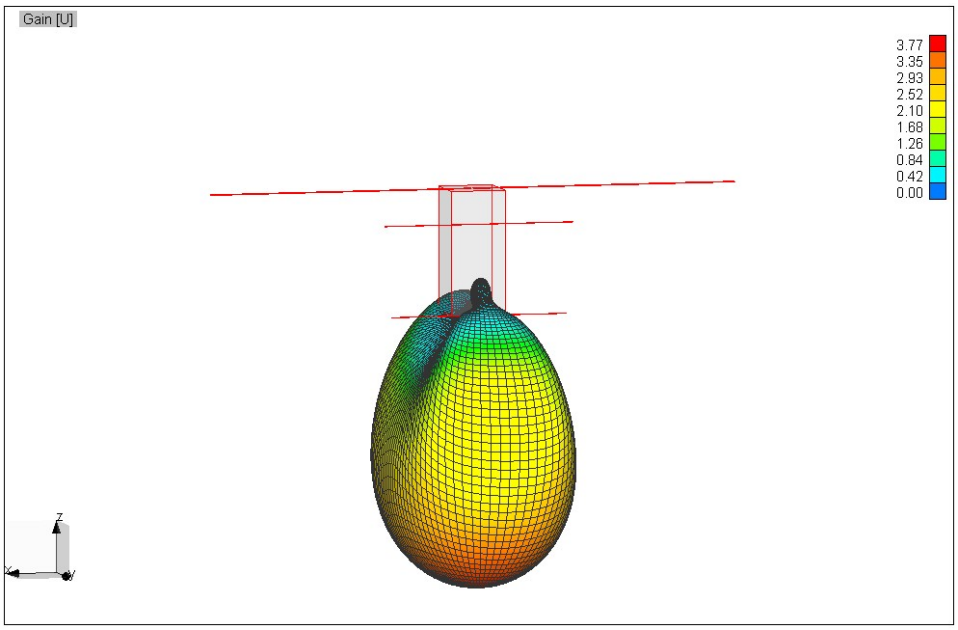

Figure 3.8: Radiation pattern of the dipole in magnitude.

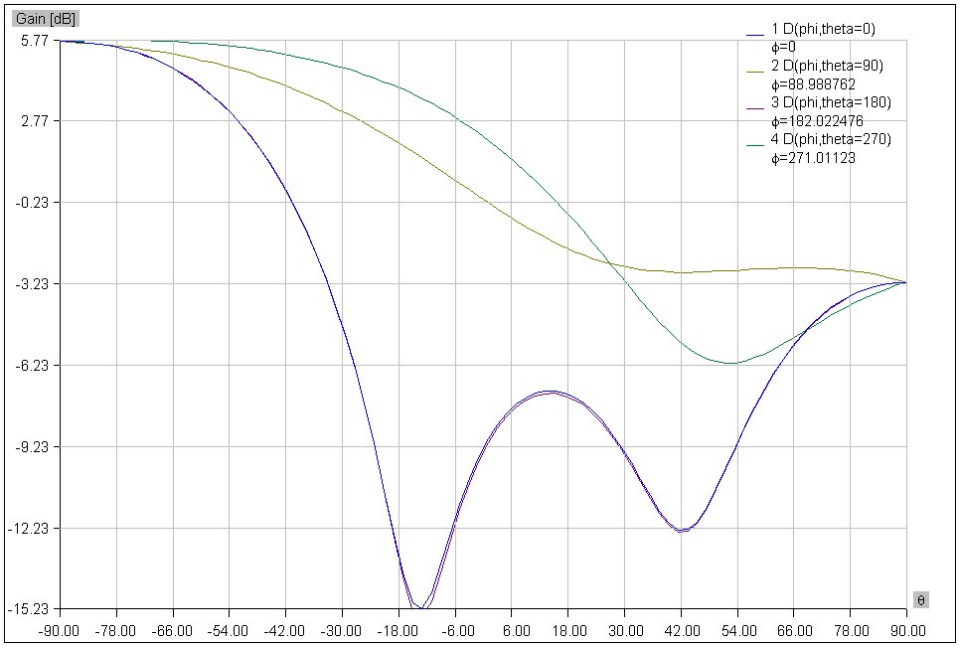

Figure 3.9: The four main radiation directions in dB

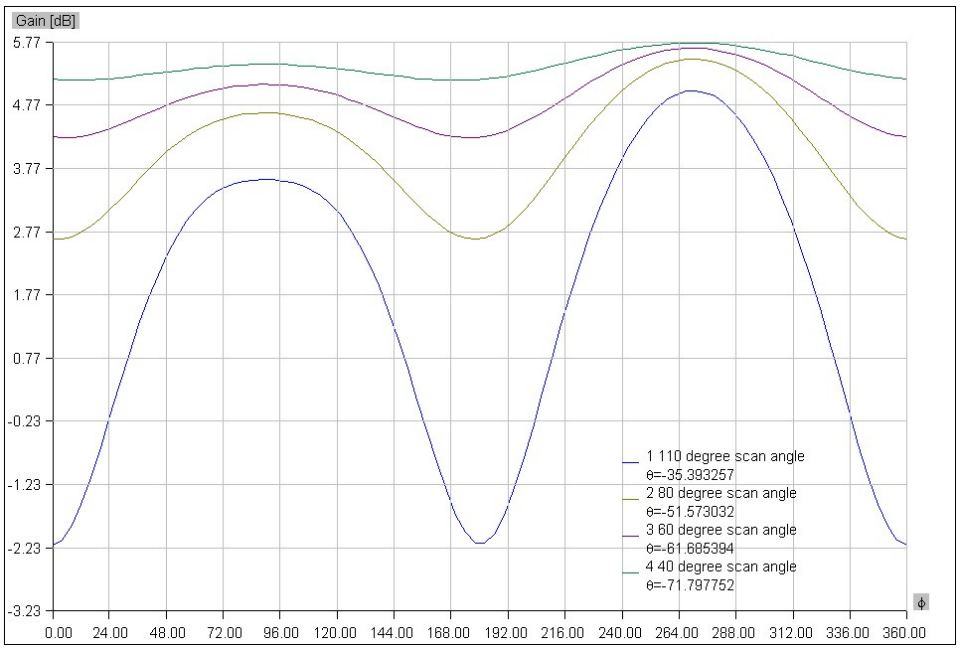

Figure 3.10: Edge gain for different scan angles

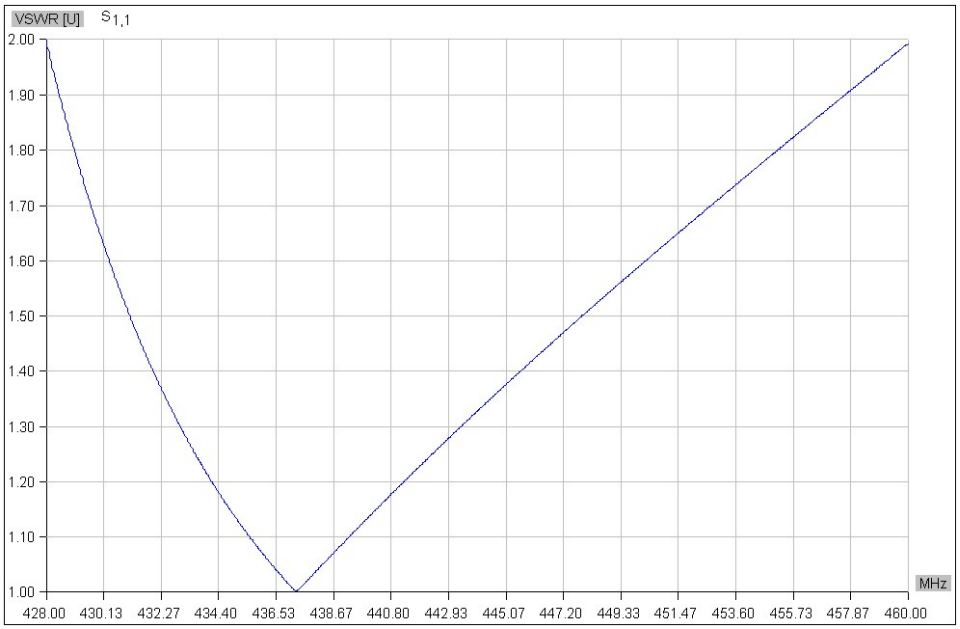

Figure 3.11: VSWR plotted for the usable bandwith of the antenna

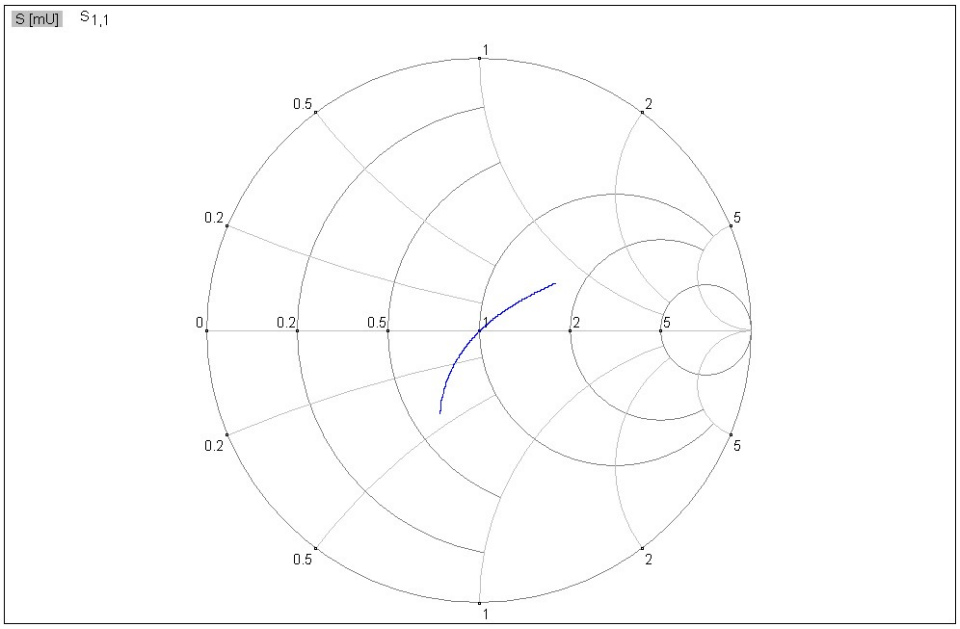

Figure 3.12: Smith chart plotted over the usable bandwith

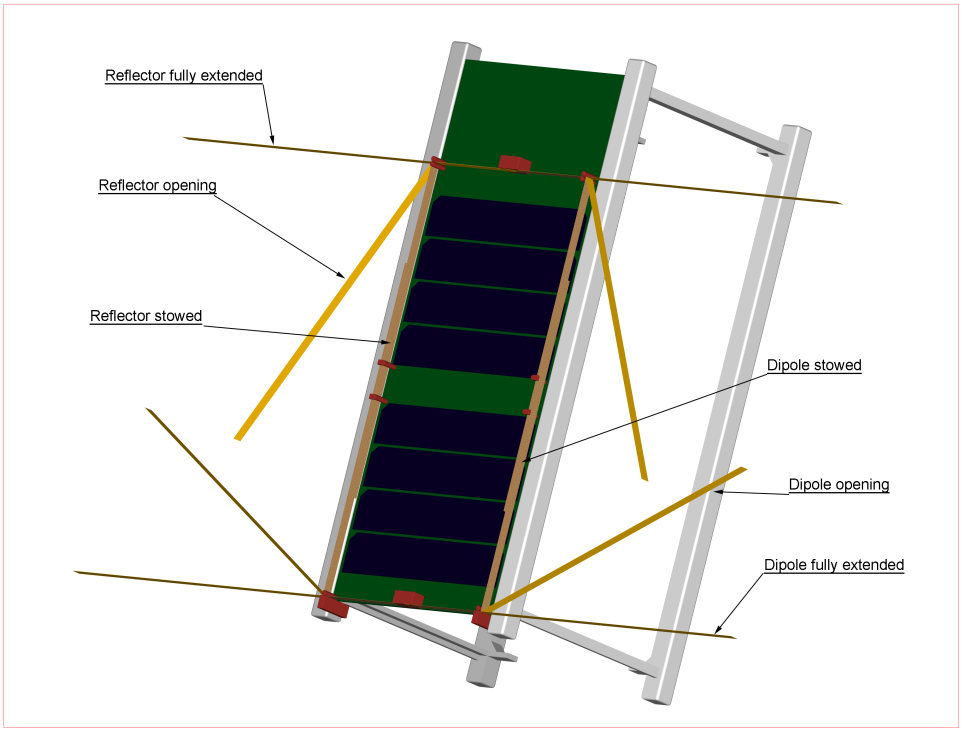

Figure 3.13: CAD drawing showing the antenna function when mounted on the front sidewall of the satellite.

Chapter 4

Discussion

The simulation showed a surprizing result in that the antenna could be tuned to an exact 50 Ω match. Although the final efficiency of the antenna is dependent on the ohmic losses in the materials chosen for the construction, this gives an exellent basis for a good realization. That the final solution is an antenna that may be used in both a fully extended, directive mode, and in a more omnidirectional mode with the reflector folded, is of particular interest. This feature enables the antenna to be used even if the satellite fails to stabilize, or if the reflector release mechanism fails, though with substancially reduced EIRP.

A broadband impedance plot is shown in figure A.4, indicating good power rejection in the 145 MHz band. This is neccesary to withstand interference from the other radio system, as it might interefere with certain radio components despite being out-of-band.

As no electrical measurements were performed on the physical model, the experimental results were only of a practical, mechanical nature. However, although crudely manufactured, the physical model proved that it is possible to construct the antenna as 4 mm wide metal sheets, and that the offset mounting solution is conforming with [3]. Because of the relatively short length of the elements, sideways curving may not be necessary to make them rigid. However, such a measuring tape-form will aid the position accuracy and rigidity of the elements when they are extended. Anchors, as illustrated in 3.13, will be needed to keep the elements in position when folded, thus some space must be reserved for this. 4 mm is therefore the likely maximum width of the elements.

The suggested release mechanism consisting of nylon threads with nichrome cutter wires, will problably be the solution best suited for this mounting. Unfortunately, a development and test of such a mechanism was not acheived due to lack of time. Two solutions stand out as possible, however: Either a single system, releasing both the dipole and reflector at once, or a stepwise release solution, in which the dipole is released first, and the reflector af-

terwards. The latter system makes possible two different antenna patterns, one directive and one omnidirectional. Both solutions can make use of the Nylon-Nichrome mechanism. In any case, redundancy shold be added in the form of two or more nichrome wires for each nylon thread to be cut.

Studies of the physical model showed that the offset solution would probably be the easiest to realize, because it allows for greater adjustment flexibility. Furthermore, in neither electrical, nor mechanical design does the internal layout of the satellite interfere with the antenna. This is certainly not the case with the center mounted solution.

Finally, it is important to note that the optimum characteristics derived in this work are valid only for an ideal case. When lossy media is used, the ideal lengths of the dipole and reflector may differ from the ideal case. However, the computer simulation is believed to be a sufficiently good approximation for making the basis of a physical test, using the constructed test model.

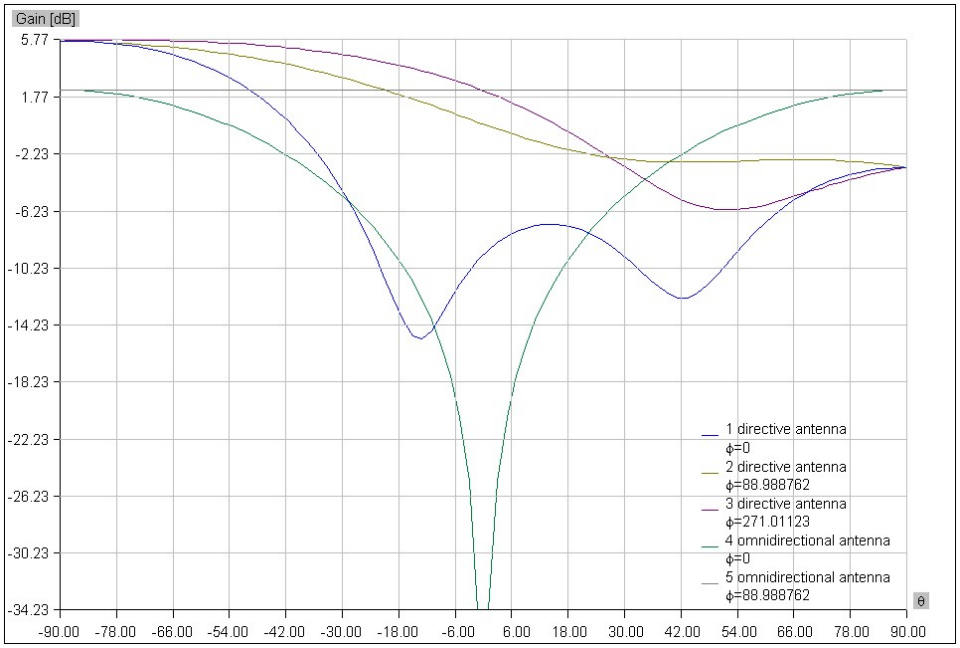

Figure 4.1: Comparison of an omnidirectional dipole optimized for 437 MHz carrier frequency, and the directive antenna. Three directions are given for th directive antenna, as it is not completely symmetric.

Figure 4.1 compares the radiation pattern of an omnidirectional dipole to the pattern of the final antenna solution. From the figure, one can draw the conclusion that the directional antenna is better than a regular dipole in any way for scan angles smaller than 125°. This angle is large enough to cover the entire earth when seen from a height of 750 km, and substancially larger than the 110° scan angle required.

Chapter 5

Conclusion

A computer model of the antenna was successfully produced, optimized and simulated. The result was a directive antenna meeting the primary design goals. A physical test model was built, but tests based on this model have been delayed for the spring of 2007.

The directive antenna yields a greater and more stable gain than an omnidirectional antenna for scan angles up to 125°. The antenna also posesses good rejection of the 145MHz band, ensuring that it will not contribute to interference from the other radiosystem in the satellite. The impedance of the antenna is a near constant 50 Ω through the required bandwith, as it only changes by about 1.5 Ω/MHz, the requried bandwith being only about 0.050 MHz. In addition, the directive antenna seems to be a perfect match to a 50 Ω feeding network, easing the electrical implemetation.

All in all, there is no doubt that the antenna is an efficient addition to the 437 MHz link budget of the satellite. The possibility for use even without the reflector extended, ensures that the radio system is not rendered useless in the event of ADCS failure or if the reflector release mechanism malfunctions. In contrast to the reflector, however, the dipole must be folded out in order for the radio system to be operational.

Work regarding the physical design and implementation of both antenna and release mechanism should is expected to be time consuming, and it is recommended that this is realized as a project assignment or master thesis involving at least one student. Such a task will demand conciderable mechanical skills and knowledge, and involvement of other institutes may be recommendable.

Bibliography

[1] Constantine A. Balanis. *Antenna Theory.* Wiley-Interscience, third edition, 2005.

[2] Roger Birkeland. 145 mhz dipole antenna for double cubesat, 2007.

[3] Cubesat design specification, revision 9, 2005.

[4] David K. Cheng. *Field and Wave Electromagnetics.* Addison Wesley, second edition, 1992.

[5] J. Allmutt T. Pratt, C. Bostian. *Satellite Communications.* John Wiley & Sons, second edition, 1986.

Appendix A

Appended Figures

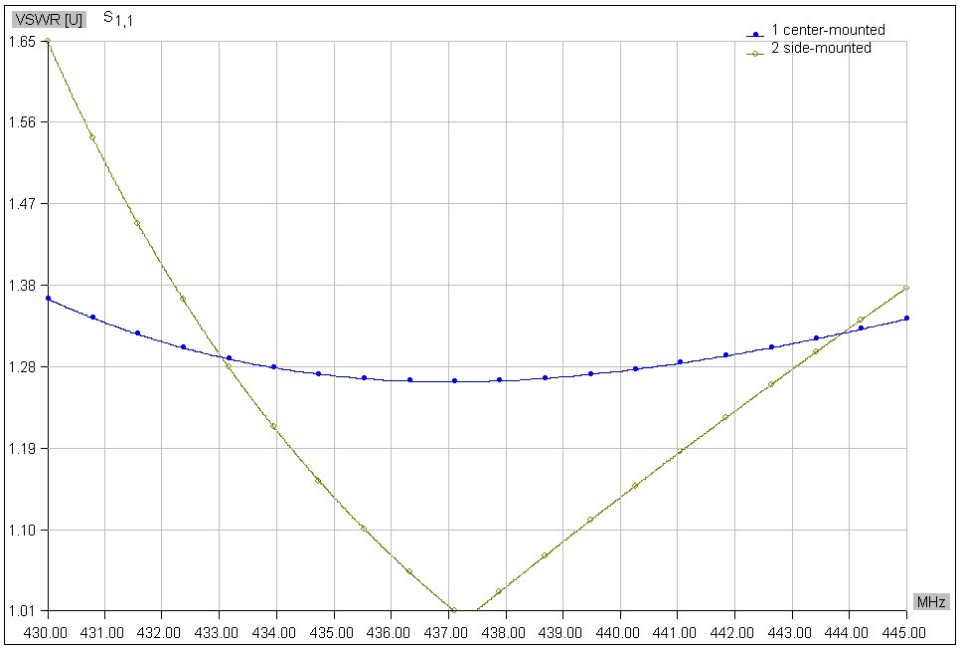

Figure A.1: Comparison of VSWR for the center and side-mounted antenna solutions. Note that the side-mounted solution has a lower VSWR for the entire releveant bandwidth.

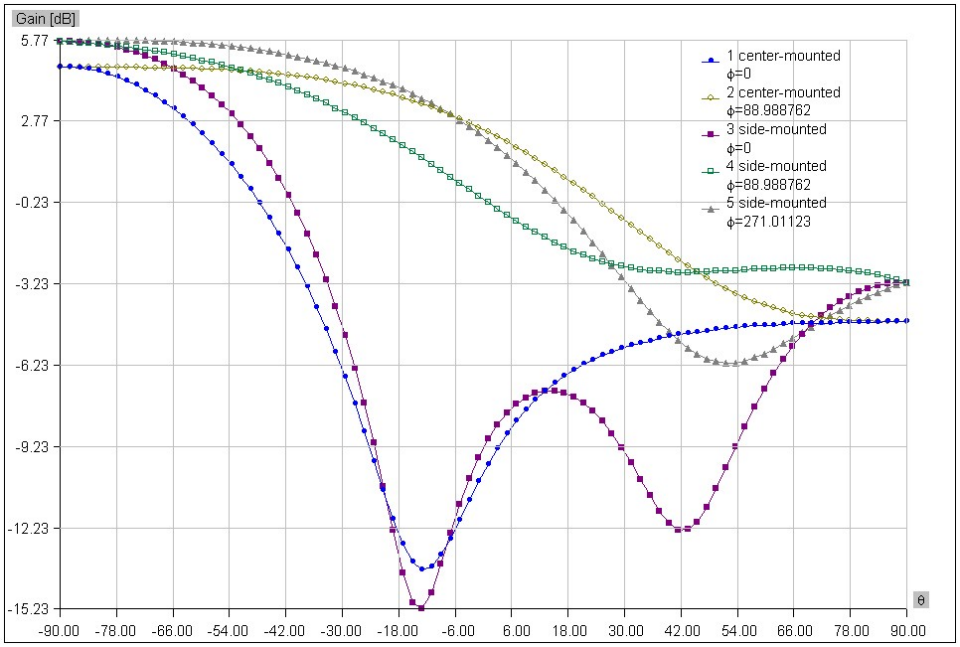

Figure A.2: Comparison of radiation patterns for the cente and side-mounted antennas. Note the non-uniformity of the side-mounted antenna, due to interference from the satellite chassis

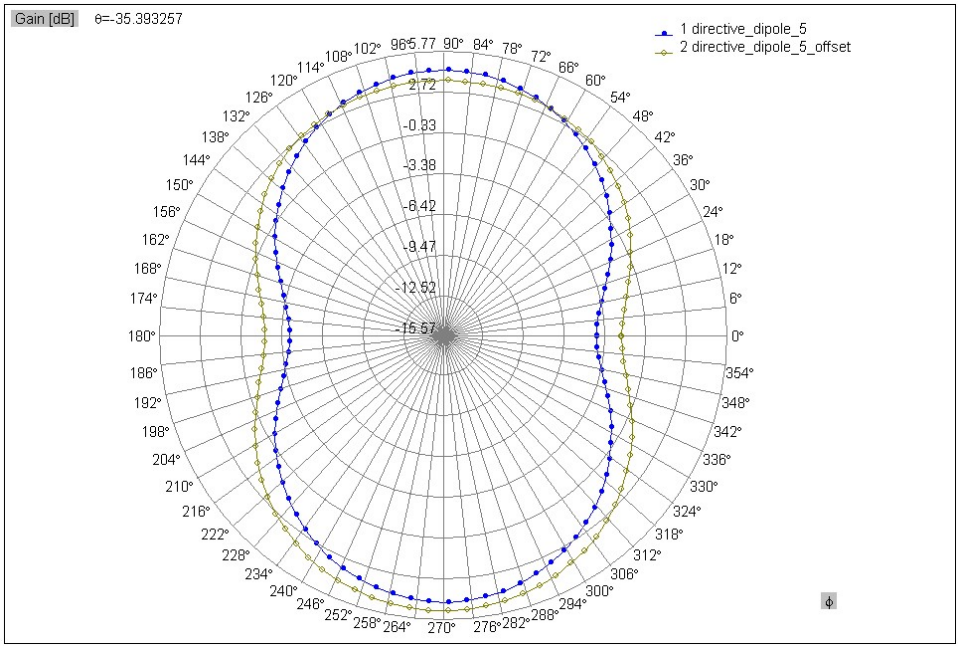

Figure A.3: Comparison of a normalized 110 degree lobe angle for the center and side-mounted solutions. Note again the non-uniformity of the side-mounted solution

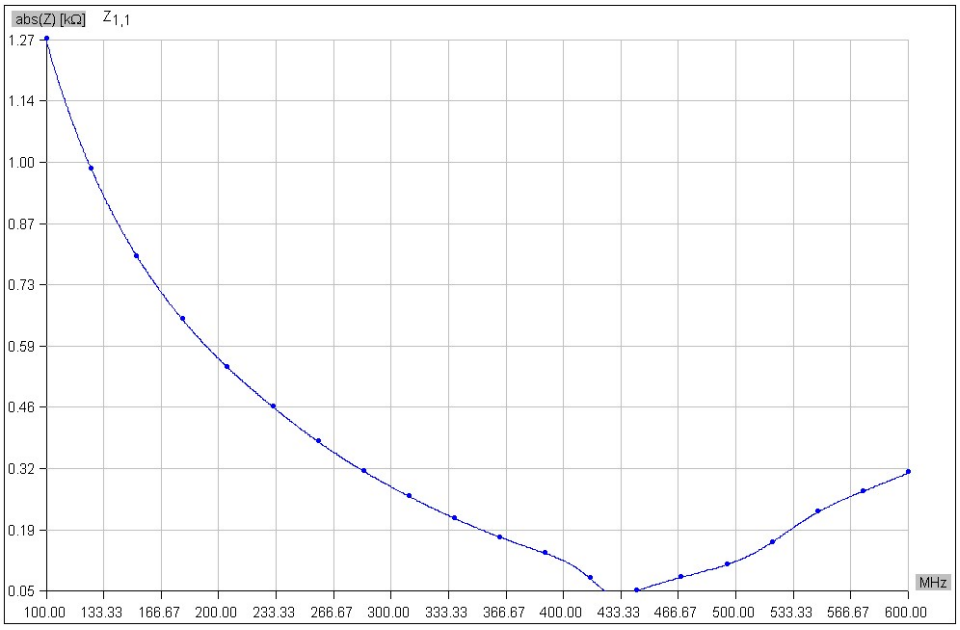

Figure A.4: Plot showing the input impedance of the antenna over a wider frequency band.

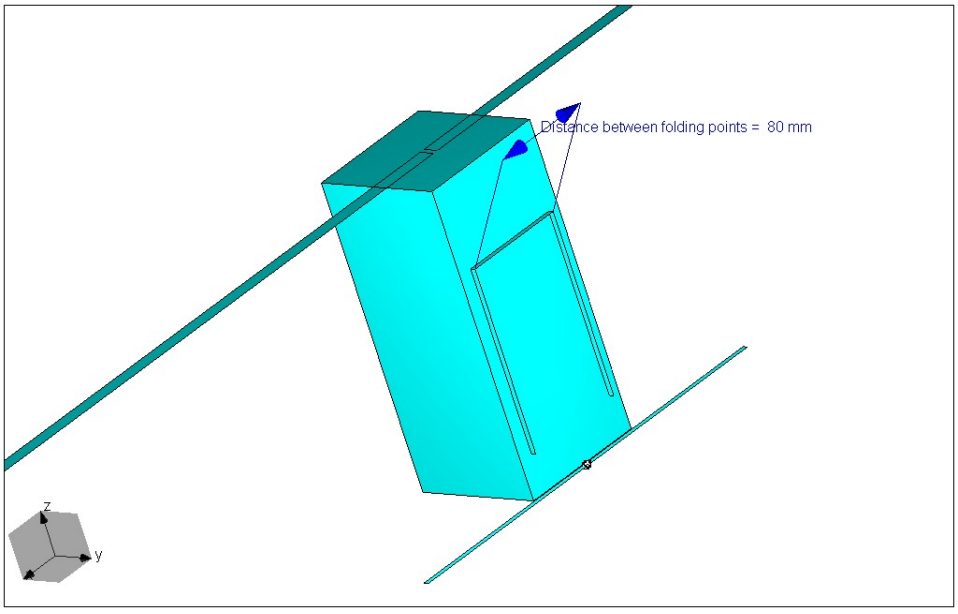

Figure A.5: Layout used to simulate the antenna properties when the reflector is folded. All measurements are the same as in the optimized case.

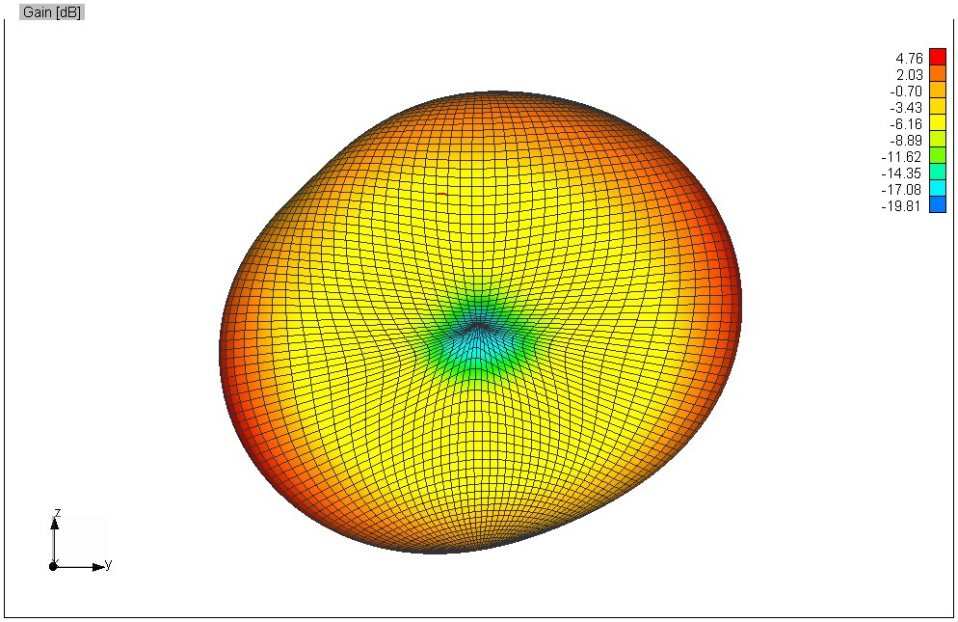

Figure A.6: Radiation pattern of the antenna when the reflector is folded

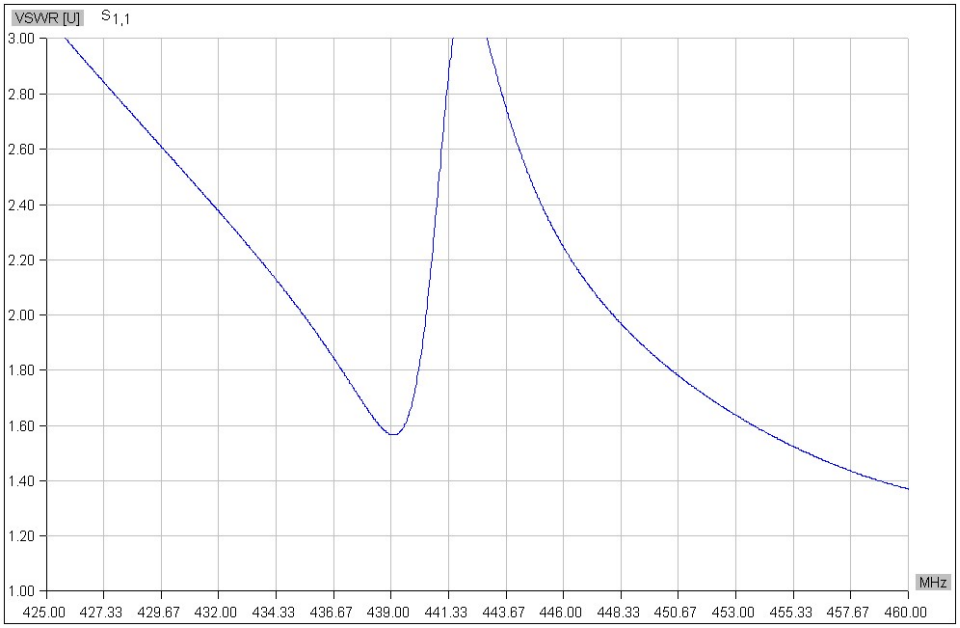

Figure A.7: VSWR of the antenna when the reflector is folded

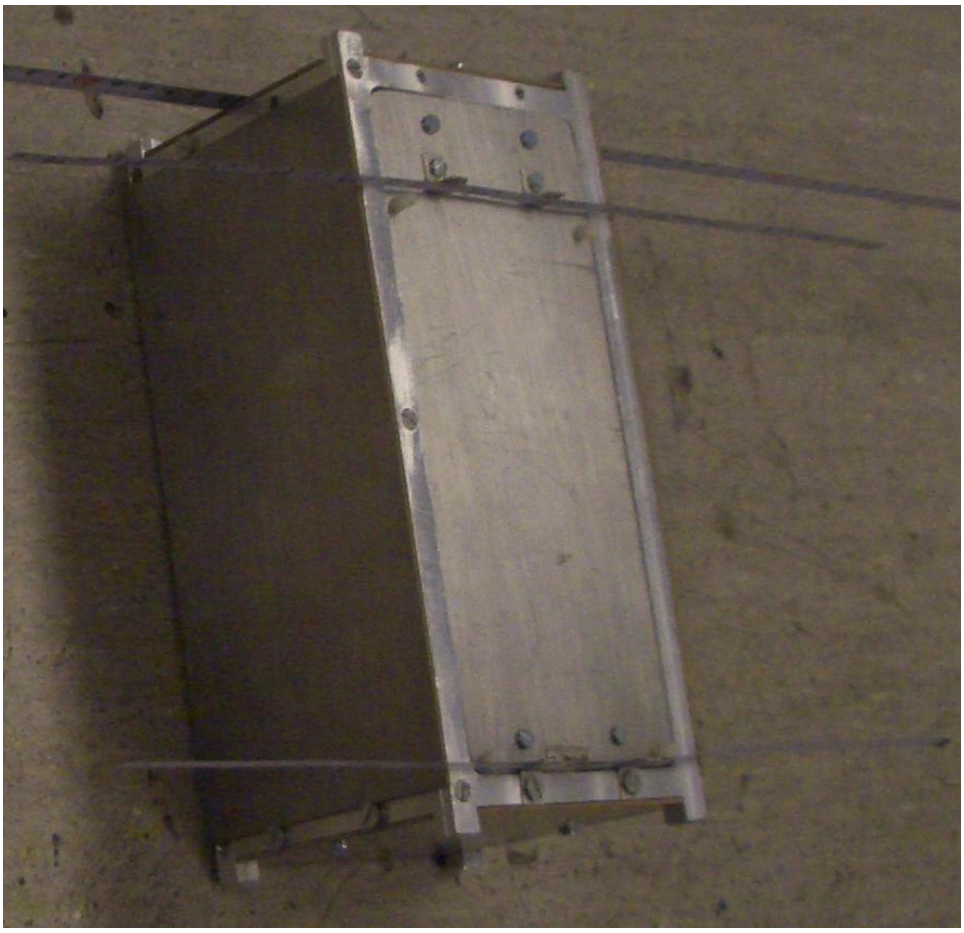

Figure A.8: The model built for testing the construction, and for measuring antenna properties.